

ARTICLE



SRSF1 plays a critical role in invariant natural killer T cell development and function

Jingjing Liu^{1,5}, Menghao You^{1,5}, Yingpeng Yao¹, Ce Ji¹, Zhao Wang¹, Fang Wang¹, Di Wang², Zhihong Qi¹, Guotao Yu¹, Zhen Sun¹, Wenhui Guo¹, Juanjuan Liu¹, Shumin Li³, Yipeng Jin³, Tianyan Zhao¹, Hai-Hui Xue^{1,4}, Yuanchao Xue² and Shuyang Yu¹✉

© The Author(s), under exclusive licence to CSI and USTC 2021

Invariant natural killer T (iNKT) cells are highly conserved innate-like T lymphocytes that originate from CD4⁺CD8⁺ double-positive (DP) thymocytes. Here, we report that serine/arginine splicing factor 1 (SRSF1) intrinsically regulates iNKT cell development by directly targeting *Myb* and balancing the abundance of short and long isoforms. Conditional ablation of SRSF1 in DP cells led to a substantially diminished iNKT cell pool due to defects in proliferation, survival, and TCR α rearrangement. The transition from stage 0 to stage 1 of iNKT cells was substantially blocked, and the iNKT2 subset was notably diminished in SRSF1-deficient mice. SRSF1 deficiency resulted in aberrant expression of a series of regulators that are tightly correlated with iNKT cell development and iNKT2 differentiation, including *Myb*, PLZF, Gata3, ICOS, and CD5. In particular, we found that SRSF1 directly binds and regulates pre-mRNA alternative splicing of *Myb* and that the expression of the short isoform of *Myb* is substantially reduced in SRSF1-deficient DP and iNKT cells. Strikingly, ectopic expression of the *Myb* short isoform partially rectified the defects caused by ablation of SRSF1. Furthermore, we confirmed that the SRSF1-deficient mice exhibited resistance to acute liver injury upon α -GalCer and Con A induction. Our findings thus uncovered a previously unknown role of SRSF1 as an essential post-transcriptional regulator in iNKT cell development and functional differentiation, providing new clinical insights into iNKT-correlated disease.

Keywords: Invariant natural killer T cell; SRSF1; Development; Function; Alternative splicing

Cellular & Molecular Immunology (2021) 18:2502–2515; <https://doi.org/10.1038/s41423-021-00766-w>

INTRODUCTION

Invariant natural killer T (iNKT) cells, also named type I or classic NKT cells, are specialized T lymphocytes that play crucial roles in both innate and adaptive immune responses [1]. These cells express the invariant T cell antigen receptor (TCR) α -chain (V α 14-J α 18 in mice, V α 24-J α 18 in humans) with a limited set of TCR β -chains [2]. Progenitors from CD4⁺CD8⁺ double-positive (DP) thymocytes are positively selected by glycolipids in complex with CD1d, an MHC-class-I-like molecule, resulting in successful lineage commitment of iNKT cells [3–5]. Based on the expression of CD24, CD44, and NK1.1, iNKT cells can be further sequentially subcategorized into four developmental stages: stage 0, stage 1, stage 2, and stage 3 [6, 7]. Given the limitations of this linear stage developmental model, iNKT cells were defined as three functional subsets in a new transcription factor (TF)-based classification, termed iNKT1 (PLZF^{lo}ROR γ t^{lo}T-bet^{hi}), iNKT2 (PLZF^{hi}ROR γ t^{lo}T-bet^{lo}), and iNKT17 (PLZF^{med}ROR γ t^{hi}T-bet^{lo}) [8]. Recently, single cell-based studies of iNKT cells have shown that both the iNKT1 and iNKT2 populations display high heterogeneity [9, 10], suggesting that the complicated regulatory mechanisms of iNKT cell development need to be further disclosed.

iNKT1 cells express the TF T-bet and predominantly secrete interferon- γ (IFN γ), which occurs in all stages of development and is

mainly found at stage 3; iNKT2 cells express TF PLZF and Gata3 and produce high levels of interleukin 4 (IL-4) at stage 2; and iNKT17 cells express TF ROR γ t and primarily secrete interleukin 17 (IL-17) at stage 2 [8]. Upon stimulation, iNKT cells secrete cytokines instantly without the need for prior activation [8, 11]. These cytokines have protective or detrimental roles in autoimmune diseases, infection, and tumor surveillance [12, 13]. Accumulating studies have demonstrated that iNKT cells not only have destructive roles in promoting liver injury but also play a novel role in orchestrating the repair process during sterile injury [14–17].

Over the years, various TFs involved in the development and function of iNKT cells have been well characterized [7, 18–20]. Promyelocytic leukemia zinc finger (PLZF; encoded by *Zbtb16*) is a master regulator of iNKT cells that is maintained at elevated levels in stages 0–2 [21, 22]. Other TFs, including *Myb* [23], ICOS [24, 25], Gata3 [26], Egr2 [27], and T-bet [28], also promote iNKT cell development, whereas Klf2 [8, 29], Id2, and Id3 [30, 31] negatively control iNKT cell differentiation. These findings indicate that regulation at the transcriptional layer is responsible for iNKT cell formation. However, post-transcriptional events that drive the iNKT cell development program remain poorly understood.

RNA-binding protein (RBP)-mediated alternative splicing (AS) has been progressively considered a major determinant in controlling

¹State Key Laboratory of Agrobiotechnology, College of Biological Sciences, China Agricultural University, Beijing, China. ²Key Laboratory of RNA Biology, Institute of Biophysics, Chinese Academy of Sciences, Beijing, China. ³Clinical Department, College of Veterinary Medicine, China Agricultural University, Beijing, China. ⁴Center for Discovery and Innovation, Hackensack Meridian Health, Nutley, NJ, USA. ⁵These authors contributed equally: Jingjing Liu, Menghao You. ✉email: ysy@cau.edu.cn

Received: 12 May 2021 Accepted: 25 August 2021

Published online: 14 September 2021

gene expression and cell fate by post-transcriptional regulation [32, 33]. Serine/arginine splicing factor 1 (SRSF1) is an archetypical RBP of the serine and arginine-rich (SR) protein family and a key splicing regulator that controls mRNA metabolism, splicing, decay, nuclear export, and translation [34]. Although SRSF1 has been extensively investigated, its function and target specificity in immune cells are still unclear.

In this study, we explored the critical requirement of SRSF1 in iNKT cells by a conditional knockout approach. Our findings reveal that SRSF1 serves as a post-transcriptional regulator of both iNKT cell development and function, indicating the therapeutic potential in iNKT-related immune disorders.

MATERIALS AND METHODS

Mice

Srsf1^{fl/fl} mice were generously provided by Dr. Xiang-Dong Fu (University of California, San Diego). The targeting strategy has been previously described [35]. *LCK-Cre* (Stock No: 006889) [36] and *B6SJL* (CD45.1⁺) mice were obtained from The Jackson Laboratory. The *Srsf1*^{fl/fl} mice and all strains used in this study had a C57BL/6 genetic background. For phenotypic and functional analysis, the mice were selected from 6- to 7-week-old littermates. For the bone marrow chimeric model, 6- to 10-week-old *B6SJL* recipients were used, and age matching was ensured for each individual experiment. Mice were kept under specific pathogen-free conditions with controlled temperature (22 ± 1 °C) and humidity (50 ± 10%) and exposed to a constant 12-h light-dark cycle in the animal facilities at China Agricultural University. All institutional and national guidelines for the care and use of laboratory animals were followed.

Cell isolation

Single-cell suspensions were prepared from the thymus and spleen as previously described [37]. For isolation of liver-derived lymphocytes, the liver was thoroughly dissected with RP10 (RPMI 1640 medium containing 10% FBS) and then filtered through a 70-µm cell strainer to obtain a single-cell suspension. Liver lymphocytes were centrifuged at 500 × *g* for 5 min, pellets were then suspended in 48% Percoll (17089101, Gentihold), and red blood cells were removed with ACK lysis buffer as previously described [38]. Mononuclear cells at the bottom of the solutions were collected for subsequent assays.

Flow cytometry

The following fluorochrome-labeled monoclonal antibodies were used: anti-TCRβ (H57-597), anti-CD24 (M1/69), anti-NK1.1 (PK136), anti-CD3e (145-2C11), anti-CD4 (RM4-5), anti-CD8a (53-6.7), anti-B220 (RA3-6B2), anti-Ly6G (RB6-BC5), anti-CD11b (M1/70), anti-CD11c (N418), anti-Ter119 (TER-119), anti-TCRγδ (GL-3), anti-CD45.2 (104), anti-CD1d (1B1), anti-PLZF (Mags.21F7), anti-RORyt (AFKJS-9), anti-T-bet (4B10), anti-Gata3 (TWAJ), anti-IFNγ (XMG1.2), and anti-IL-4 (11B11) were from eBioscience; anti-CD44 (IM7), anti-CD45.1 (A20), and anti-IL-17A (TC11-18H10) were from BD Biosciences; anti-ICOS (C398.4A) was from BioLegend; and anti-CD5 (53-7.3) was from Abcam. For surface staining, cells were stained with PBS57/CD1d tetramer, followed by staining with the corresponding antibodies in FACS buffer (PBS + 2% FBS). For intranuclear staining of the transcription factors PLZF, T-bet, Gata3, and RORyt, cells were fixed and permeabilized with Foxp3/Transcription Factor Staining Buffer Set (00-5523-00, Thermo Fisher Scientific) following the manufacturer's instructions. For the analysis of cytokines, including IFNγ, IL-17A, and IL-4, cells were fixed and permeabilized with a Cytofix/Cytoperm Fixation/Permeabilization Solution Kit (554714, BD Biosciences). Samples were acquired with FACSVerse or LSRFortessa (BD Biosciences) following the manufacturer's instructions. Cell sorting was performed with a FACSAria II sorter (BD Biosciences) as previously described [39]. The flow cytometry data were analyzed with FlowJo software (Version 10.4.0, Tree Star, Inc.).

Detection of cytokines in vitro

For analysis of cytokine secretion of thymic iNKT cells, thymocytes were stimulated in vitro with PMA (100 ng/ml) and ionomycin (50 µg/ml) diluted in RPMI medium supplemented with 10% FBS, GolgiStop (1000×, 554724, BD Biosciences), and GolgiPlug (1000×, 555029, BD Biosciences) for 4 h. Cells were washed, stained with surface markers, and fixed with BD Cytofix/Cytoperm (554722, BD Biosciences), followed by intracellular staining with anti-IFNγ, anti-IL-4, and anti-IL-17A.

In vivo BrdU incorporation and apoptosis assays

For determination of the proliferation rate of iNKT cells, mice were injected *i.p.* with 1 mg BrdU (B5002, Sigma) in 200 µl of PBS at 0, 24, and 48 h. Then, the mice were euthanized at 72 h post-injection, and single-cell suspensions were collected from relevant tissues [40]. Thymocytes were surface stained with relative antibodies, fixed, and permeabilized as described above. BrdU incorporation was measured using a BrdU Flow Kit (557891, BD Biosciences) according to the manufacturer's instructions.

For apoptosis detection, single-cell suspensions were stained with surface markers and resuspended in Annexin V binding buffer (BD Biosciences) containing fluorochrome-conjugated Annexin V (BMS306F1/300, eBioscience). Apoptotic cells were measured according to the manufacturer's instructions.

Bone marrow chimeric mice

Bone marrow chimeras were generated as previously described [37]. Briefly, bone marrow (BM) cells from femurs and tibias were harvested and mixed at a 1:1 ratio with *B6SJL* (CD45.1⁺) bone marrow cells as donors for chimeric mice. A total of 2 × 10⁶ donor cells were injected intravenously into lethally irradiated (8 Gray) *B6SJL* recipients. Chimeric mice were analyzed 9 weeks post-transplantation.

Retroviral transduction

The full-length CDS encoding the short isoform of Myb (Myb^{p75}) or long isoform of Myb (Myb^{p89}) was cloned into the pMigR1 vector for retroviral gene transduction. For the retrovirus package, HEK293T cells were transfected with the indicated plasmids by Lipofectamine 3000 (L3000015, Invitrogen) [41]. Briefly, retroviruses bearing Myb^{p75}, Myb^{p89}, or pMigR1 along with pCL-Eco were packaged with HEK293T cells and collected at 48 and 72 h after transfection. The retrovirus-containing medium was filtered through 0.45 µm filters and loaded onto 24-well nontissue culture plates (351147, Falcon) precoated with 10 µg/well RetroNectin (T100A, TaKaRa). Next, BM cells were isolated from ctrl or *LCK*^{Cre/+}*Srsf1*^{fl/fl} mice (CD45.2⁺) and then stained with a biotinylated lineage-positive antibody cocktail (anti-CD45R, anti-Ly6G, anti-Ter119, anti-CD11b, anti-CD11c, anti-NK1.1, anti-CD3e, anti-CD4, anti-CD8, anti-TCRγδ) followed by depletion with Dynabeads™ M-280 Streptavidin (60210, Invitrogen). Lineage-negative BM cells were cultured overnight in IMDM containing 15% FBS, 100 µg/ml streptomycin and penicillin, 50 µM 2-mercaptoethanol, 20 ng/ml TPO (315-14, PeproTech), and 50 ng/ml SCF (250-03, PeproTech) on the plate described above. Then, the cells were centrifuged at 1000 × *g* for 90 min at 30 °C in the presence of 8 µg/ml polybrene (H9268, Sigma). After spinofection, the cells were cultured at 37 °C in a 5% CO₂ incubator for another 2 h and then replaced with full IMDM containing the components and cytokines described above for 24–48 h. The infected cells containing 2000–5000 GFP⁺ cells were sorted and transplanted into irradiated (7.5 Gray) *B6SJL* mice. The recipients were analyzed at 10 weeks post-transplantation.

RNA isolation, reverse transcription, and quantitative RT-PCR

Cells were lysed by TRIzol (Invitrogen), and total RNA was extracted using a modified protocol with an RNeasy Mini Kit (74106, Qiagen) or RNeasy Micro Kit (74004, Qiagen). RNA was then reverse transcribed using a FastKing RT Kit (with gDNase) (KR106, Tiangen) following the manufacturer's instructions. Relative gene expression levels were analyzed by quantitative RT-PCR (qPCR) with SYBR Green Master Mix (Tiangen) on a CFX96 Connect™ Real-Time System (Bio-Rad). *Hprt1* was used to normalize the expression of other genes, and the 2^{-ΔΔCT} method was used to calculate the levels of target mRNAs. All primers used are listed in Table S2.

TCR rearrangement assay

The 7AAD⁻CD4⁺CD8⁺DP thymocytes were sorted from the thymi of *LCK*^{Cre/+}*Srsf1*^{fl/fl} and ctrl mice. Total RNA was extracted and reverse transcribed as described above. The cDNA transcripts were assessed by qPCR with the forward primers *Va14*, *Va8*, and *Va3* paired with the reverse primers *Ja56*, *Ja18*, *Ja9*, or *Ca* (primer sequences are listed in Table S2). The relative expression of each PCR product (after normalization to *Hprt1*) in cells from the ctrl mice was arbitrarily set to one, and its relative expression in cells from *LCK*^{Cre/+}*Srsf1*^{fl/fl} mice was normalized accordingly.

Semiquantitative PCR analysis

The cDNA was subjected to semiquantitative PCR with the defined parameters: the initial denaturation was set at 95 °C for 2 min, followed by

the indicated cycles (iNKT, 35 cycles; DP, 33 cycles; cell line, 33 cycles), including denaturation (30 s at 94 °C), annealing (30 s at 59 °C), and extension (30 s at 72 °C). For analysis of the PCR product, 1.5% agarose gels were used to separate the two isoforms, and the levels of the two isoforms were measured by Image Lab Software (Version 5.1, Bio-Rad). Each sample was assayed at least three times to ensure reliability. The primer sequences were as follows: *Myb*, 5'-CAAGGTGCATGATCGTCCAC-3' and 5'-GTCTGGTCTCGACATGGTGT-3'.

Splicing detection in vitro by minigene assays

For generation of the *Myb* minigene plasmid for alternative splicing analysis in vitro, a 3442bp DNA fragment from exon 9 to exon 10 (chr10:21,142,993–21,146,434, mm10) of the *Myb* gene was amplified directly by PCR from genomic DNA and then cloned into the pcDNA3.1 vector (V79020, Thermo Fisher Scientific) by using the BamHI and XhoI sites. The plasmid containing the mutant binding site of the *Myb* minigene described above was made by overlap-extension PCR. For generation of the expression plasmid of *Srsf1*, HA-tagged primer sets were used to amplify the coding region of *Srsf1*, and the PCR product was cloned into the pcDNA3.1 vector by using the EcoRI and XbaI sites. HEK293T cells were transfected with the *Srsf1*-expressing plasmid together with the indicated minigene plasmids using Lipofectamine 2000 following the manufacturer's instructions. Cells were harvested for RNA or protein analysis at 48 h post-transfection. Semiquantitative PCR was performed with primers for amplifying the indicated transcripts, and the desired DNA products were isolated and sequenced for further confirmation.

Western blot

Western blot analyses were carried out as previously described [37]. Briefly, 7AAD⁻CD4⁺CD8⁺DP cells were isolated from the thymi of *LCK^{Cre/+}Srsf1^{fl/fl}* and ctrl mice. Total protein was isolated from cells by lysis with ice-cold RIPA buffer. Equal amounts of protein were resolved by 10% SDS-PAGE (Invitrogen) and transferred onto PVDF membranes using an iBlot (Cat #IPVH00010, Merck Millipore). Membranes were blocked with 5% milk in TBS containing Tween-20 (Sigma-Aldrich) and immunoblotted with anti-Myb (05-175, Sigma) and anti-GAPDH (#5174, Cell Signaling Technology), followed by goat anti-rabbit IgG-HRP (ZB-2301, ZSGB-BIO) secondary antibodies. Protein bands were developed by incubation with Immobilon Western Chemiluminescent HRP Substrate (Cat #WBKLS0100, Merck Millipore).

Murine hepatitis model

For the induced liver injury model, mice were injected *i.v.* with PBS-dissolved Con A at a sublethal dose of 15 mg/kg or with 30 ng α -GalCer (KRN7000, Enzo Life Science) dissolved in PBS with 0.5% Tween-20 (vehicle). At the indicated time points, the mice were sacrificed, and serum was collected. The levels of IL-4, IFN γ , and TNF α in serum were measured by ELISAs. ALT and AST in the serum from the α -GalCer-induced or Con A-induced mice were measured by an automatic biochemical analyzer (Cobas6000, Roche) according to the manufacturer's instructions. Liver tissues were fixed in formaldehyde solution and analyzed with H&E (hematoxylin and eosin) staining. For the survival rate, mice were injected *i.v.* with a lethal dose of Con A (30 mg/kg) and monitored every 30 min after administration.

ELISA

Analysis of the serum levels of cytokines was performed by enzyme-linked immunosorbent assay kits purchased from Biolegend according to the manufacturer's protocol. Briefly, a standard sandwich ELISA, antibody-antigen-antibody, was used to assess TNF α , IL-4, and IFN γ levels in serum. The serum was coated in a 96-well plate pretreated with capture antibodies, followed by incubation with detection antibodies and avidin-HRP solution. Then, the samples were incubated with TMB Substrate Solution, and the reaction was finally blocked with Stop Solution. The absorbance at 450 nm was measured with a microplate reader (Tecan).

RNA sequencing and data analysis

Total RNA was extracted from the 7AAD⁻CD4⁺CD8⁺ DP cells of *LCK^{Cre/+}Srsf1^{fl/fl}* and ctrl mice. Then, the RNA samples were subjected to paired-end RNA-Seq using an Illumina HiSeq Xten platform. The paired-end reads were assessed for quality using FastQC (version 0.11.5); adaptors and low-quality reads were trimmed by Trimmomatic 0.36. Next, clean reads were mapped to

the mm10 mouse reference sequence using STAR (version 0.6.1). Differentially expressed genes (DEGs) were analyzed in R using DESeq2 (version 1.24.0). Significant DEGs were detected according to the following criteria: $P < 0.001$ and $|\log_2FC| > 0.5$. Gene Ontology term enrichment analysis was performed by DAVID 6.7 (<https://david.ncifcrf.gov>).

For the analysis of alternative splicing, rMATS (version 4.0.2) was used to calculate the five different categories of AS events: skipped exons (SE), retained introns (RI), mutually exclusive exons (MXE), alternative 5' splice sites (A5SS), and alternative 3' splice sites (A3SS). Significantly differentially expressed AS events were defined for those with an $FDR < 0.0001$ and $|\text{InclLevelDifference}| > 0.05$. For visualization purposes, Sashimi plots of the IGV genome browser were used to plot RNA-Seq densities along exons and junctions for multiple samples. RNA-Seq data were deposited in the Gene Expression Omnibus under accession number GSE156013.

scRNA-Seq data and ImmGen gene expression analysis

Single-cell sequencing data of thymic iNKT cells were downloaded from published scRNA-seq data (GSE152786). Data analysis was performed using functions available in the *Seurat* (v3.1.4) package of R as described by Krovi et al. [9].

Relative expression of *Srsf1* and selected genes in T and iNKT cell populations (Fig. 1A) were analyzed by publicly available data from the Immunological Genome Project (ImmGen) gene expression database (GSE15907).

Statistical analysis

Statistical analysis was performed using Prism 7.0 (GraphPad Software), and the error bar is shown as the mean \pm SD. For normally distributed data, statistical significance was determined by unpaired two-sided Student's *t* test. For analysis of groups that showed differing variance, an unpaired two-sided Welch's *t* test was used. For multiple comparisons, statistical analysis was performed by one-way ANOVA. Kaplan–Meier analysis was used, and the log-rank test was employed to determine any significant difference between the survival curves of the two groups. Statistical significance was considered as follows: * $P < 0.05$; ** $P < 0.01$; *** $P < 0.001$. NS (nonsignificant) was defined as $P \geq 0.05$.

RESULTS

SRSF1 exhibits dynamic expression in iNKT cell subsets and binds iNKT-related genes

We recently reported that conditional ablation of SRSF1 from the DP stage resulted in impaired conventional T cell development. Given that iNKT cells also originate from DP thymocytes, we wondered whether SRSF1 plays a critical role in iNKT cell development and differentiation. We thus examined the expression of *Srsf1* from DP and various T cell populations by analyzing published data (GSE15907) from the ImmGen database (Fig. 1A). Compared with other iNKT genes, *Srsf1* exhibits dynamic expression in iNKT cells and reaches a peak in the CD44⁺NK1.1⁻ and CD44⁺NK1.1⁻ iNKT subsets. Moreover, we performed a *Srsf1* expression assay in distinct clusters from recently published single-cell RNA-seq data (GSE152786) [9]. The results indicated that *Srsf1* is dynamically expressed and exhibits relatively high abundance in Clusters 0 (stage 0), 1, 2, and 3 (belonging to iNKT2 subsets), which is in accordance with the result from the analysis of the ImmGen data above (Fig. 1B). We further found that 60 genes involved in iNKT cell development and function were directly bound by SRSF1 (Fig. 1C) through overlapping analysis of iNKT cell regulatory genes (collected from published literatures, Table S1) with our CLIP-seq data in thymocytes (GSE141349). These data collectively indicated the potential roles of SRSF1 in regulating iNKT cells.

SRSF1 is essential for iNKT cell development

To extensively elucidate the function of SRSF1 in iNKT cells, we bred *Srsf1^{fl/fl}* mice [35] with *LCK^{Cre/+}* mice (JAX: 006889) [36] for conditional ablation of SRSF1 from DP thymocytes, which are the origin of iNKT cells. The deletion efficiency was further confirmed in both DP and iNKT cells (Fig. 2A). We next evaluated the iNKT cell

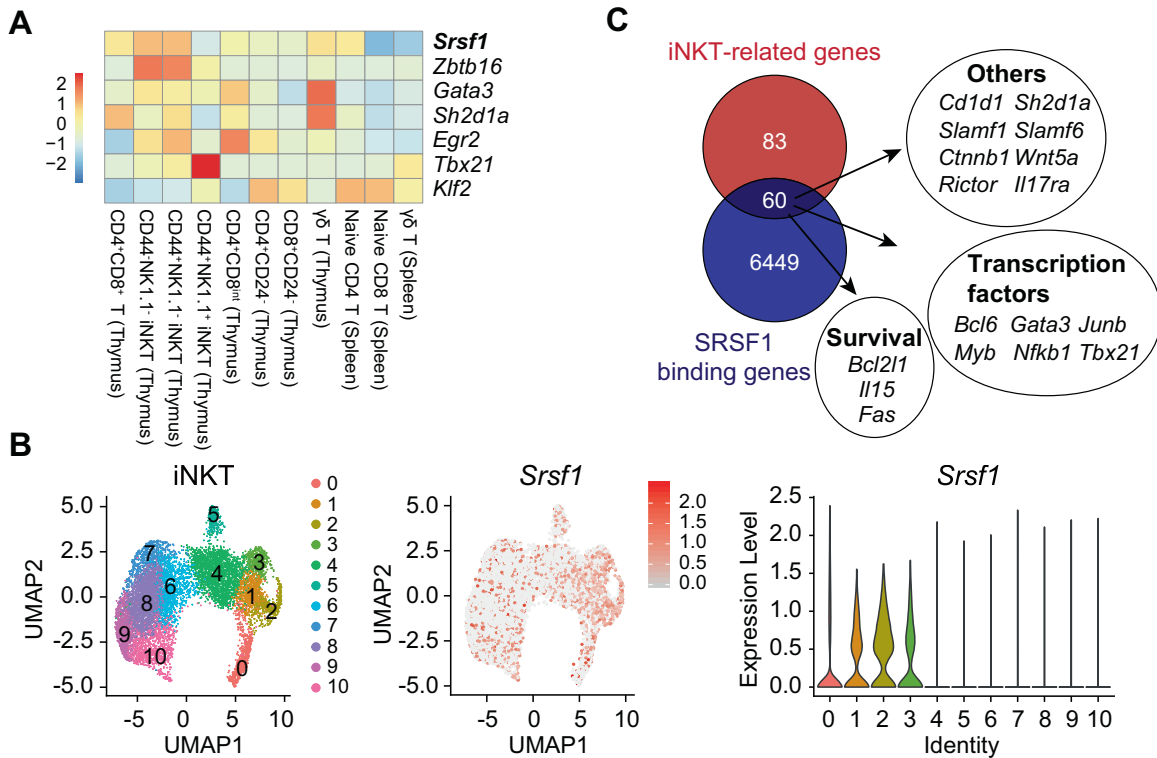


Fig. 1 SRSF1 is dynamically expressed in iNKT cell subsets and potentially binds multiple iNKT-related genes. **A** Analysis of *Srsf1* expression in various T cell subsets by published microarray data (GSE15907). **B** The expression level of *Srsf1* in thymic iNKT cells is illustrated in dot plots by published single-cell RNA-seq data (GSE152786). Left: Uniform manifold approximation and projection (UMAP) of iNKT cells was colored by inferred cluster identity; middle: The expression of *Srsf1* is plotted along a colorimetric gradient, with red corresponding to high expression; right: Violin plots showing the aggregate expression level of *Srsf1* from Cluster 0 to Cluster 10. **C** Overlapping SRSF1-binding genes in thymocytes (GSE141349) and iNKT-related genes. Sixty overlapping genes were identified, and iNKT-associated regulators in each category are shown

populations in the thymus, spleen, and liver from the $LCK^{Cre/+}Srsf1^{fl/fl}$ mice and their littermate $Srsf1^{fl/fl}$ controls (henceforth called ctrl). The frequency and numbers of iNKT cells in all these tissues from the SRSF1-deficient mice exhibited a remarkable reduction (Fig. 2B, C). The absolute numbers of stage 0 iNKT cells were significantly decreased in the $LCK^{Cre/+}Srsf1^{fl/fl}$ thymi, although the frequency of cells in stage 0 was increased (Fig. 2D, E). However, the frequency and numbers of thymic iNKT cells from stage 1 to stage 2 were significantly decreased in the $LCK^{Cre/+}Srsf1^{fl/fl}$ mice. Accordingly, the numbers of stage 3 iNKT cells were also diminished even though their frequency was not changed (Fig. 2D, E). Moreover, the numbers of iNKT cells at stages 1–3 in the periphery, such as spleens and livers, from the $LCK^{Cre/+}Srsf1^{fl/fl}$ mice were substantially diminished (Supplementary Fig. 1A, B). Given that stage 2 cells are predominantly $CD4^+$ and stage 3 cells are mostly $CD4^-$ [42], we detected CD4 expression accordingly. Reduced frequency and absolute numbers of $CD4^+$ iNKT cells were observed in thymi (Fig. 2F, G), spleens, and livers (Supplementary Fig. 1C, D). Collectively, these data demonstrated that SRSF1 is crucial for the development of iNKT cells.

SRSF1 modulates iNKT cell development in a cell-intrinsic manner

Next, we found that the expression level of CD1d in DP thymocytes was comparable between the $LCK^{Cre/+}Srsf1^{fl/fl}$ and ctrl mice (Supplementary Fig. 2A, B), reflecting that SRSF1 is dispensable for the expression of CD1d in DP thymocytes, which provides a microenvironment to support the positive selection of iNKT cells [7]. We further determined whether SRSF1 intrinsically controls iNKT cell development by using bone marrow chimeric mice as described in Supplementary Fig. 2C.

Donor-contributed iNKT cells from recipients were analyzed at 9 weeks post-transplantation. We found that the SRSF1-deficient donor cells developed fewer iNKT cells in the thymus, spleen, and liver than the control cells (Supplementary Fig. 2D, E). In addition, the frequency of iNKT cells derived from the $LCK^{Cre/+}Srsf1^{fl/fl}$ donors (presenting as $CD45.1^-$) at stages 1 to 3 in thymi (Supplementary Fig. 2F, G) was substantially reduced compared with those from the ctrl donors, as well as in spleens and livers (Supplementary Fig. 2H, I). Together, these results indicated a cell-intrinsic requirement of SRSF1 for iNKT cell development.

SRSF1 controls the differentiation of iNKT functional subsets

We next investigated whether iNKT functional subsets were affected in the SRSF1-deficient mice. The frequency and numbers of iNKT2 cells in the thymus were significantly impaired in the $LCK^{Cre/+}Srsf1^{fl/fl}$ mice (Fig. 3A, B). Although the frequency of iNKT1 cells was not altered and the frequency of iNKT17 cells was significantly increased, the absolute numbers of both subsets were notably reduced in thymi due to diminished total numbers of iNKT cells (Fig. 3A, B). The numbers of iNKT cells in all subsets of spleens from the $LCK^{Cre/+}Srsf1^{fl/fl}$ mice were notably diminished (Supplementary Fig. 3). These defects in functional differentiation may be partially caused by reduced expression of the essential regulators PLZF, Gata3, ICOS, and CD5 in relative developmental stages (Fig. 3C, D). Accordingly, the SRSF1-deficient iNKT cells showed severely reduced IL-4 production due to diminished iNKT2 cell proportions after 4 h of stimulation with PMA and ionomycin, but no significant difference in the percentages of IFN γ and IL-17A was observed (Fig. 3E, F). These data demonstrated that SRSF1 is required for the functional differentiation of iNKT cells.

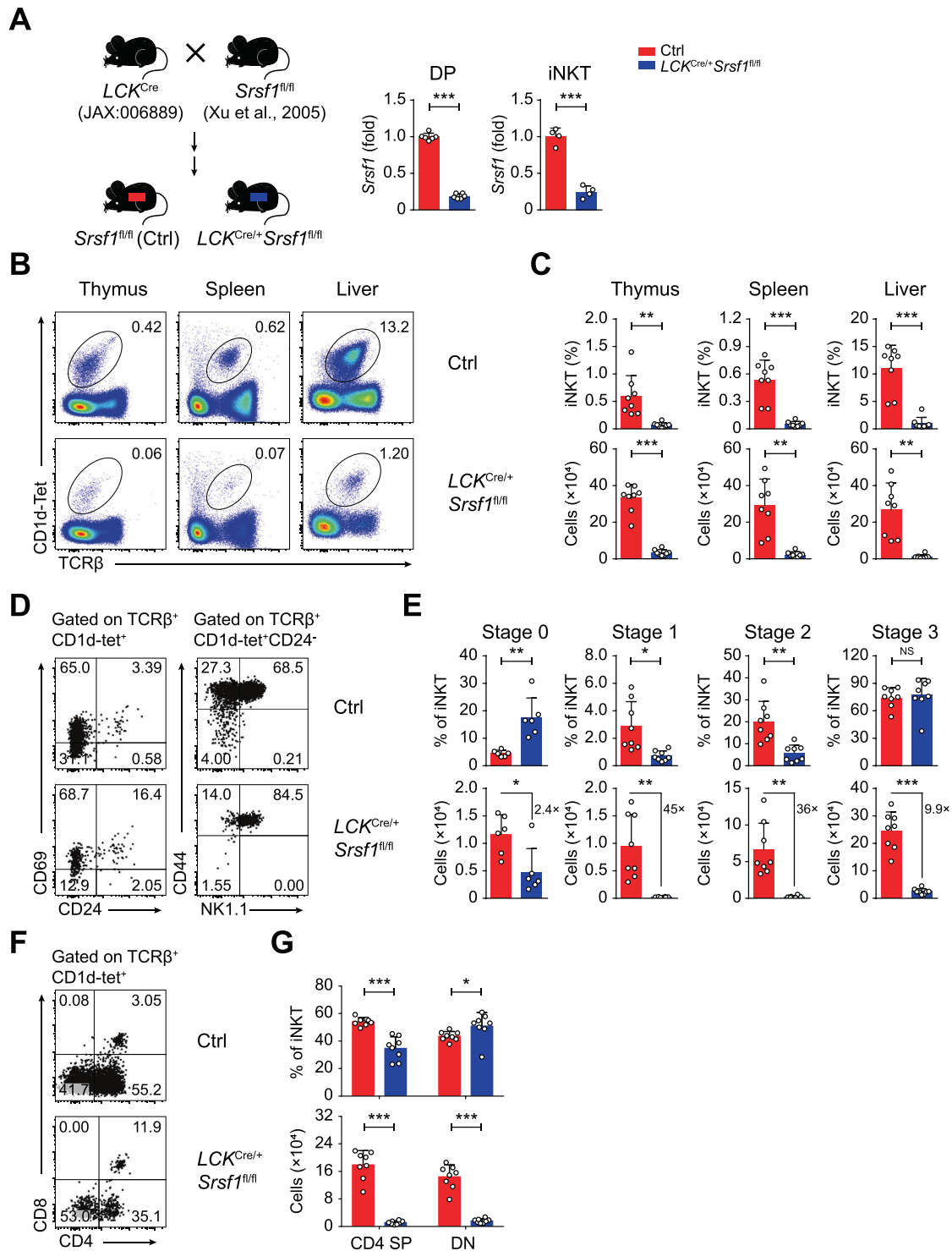


Fig. 2 Ablation of SRSF1 impairs the development of iNKT cells. **A** Schematic graphs showing the strategy for generating the mouse model (left). The source of each strain was marked. The *LCK^{Cre/+}Srsf1^{fl/fl}* mice with conditional ablation of SRSF1 and littermate *Srsf1^{fl/fl}* mice (ctrl) were used throughout the study. *Srsf1* mRNA expression in thymic DP and iNKT cells (right) was analyzed with qPCR. The relative expression of *Srsf1* (after normalization to *Hprt1*) in cells from the ctrl mice was arbitrarily set to one, and its relative expression in cells from the *LCK^{Cre/+}Srsf1^{fl/fl}* mice was normalized accordingly ($n \geq 4$). **B**, **C** Representative pseudocolor plots (**B**) showing TCRβ⁺CD1d-Tet⁺ iNKT cells from thymi, spleens, and livers. The frequency and numbers of each population are shown in (**C**) ($n = 8$). **D**, **E** Developmental stage analysis. A representative dot plot (**D**) shows CD24 and CD69 expression in total thymic iNKT cells; TCRβ⁺CD1d-Tet⁺CD24⁻ cells were further analyzed by CD44 and NK1.1. The frequency and numbers of each stage are shown in (**E**) ($n \geq 6$). **F**, **G** Flow cytometric analysis of CD4 and CD8 expression among TCRβ⁺CD1d-Tet⁺ cells in the thymus of the ctrl and *LCK^{Cre/+}Srsf1^{fl/fl}* mice (**F**). Frequency and cell numbers of each subset were shown in (**G**) ($n = 8$). Data were pooled from at least three independent experiments. Statistical significance was determined by unpaired two-sided Student's *t* test for normally distributed data, or an unpaired two-sided Welch's *t* test was used when the variance between the groups was unequal. * $P < 0.05$; ** $P < 0.01$; *** $P < 0.001$; NS denotes not significant. Data are the mean ± SD

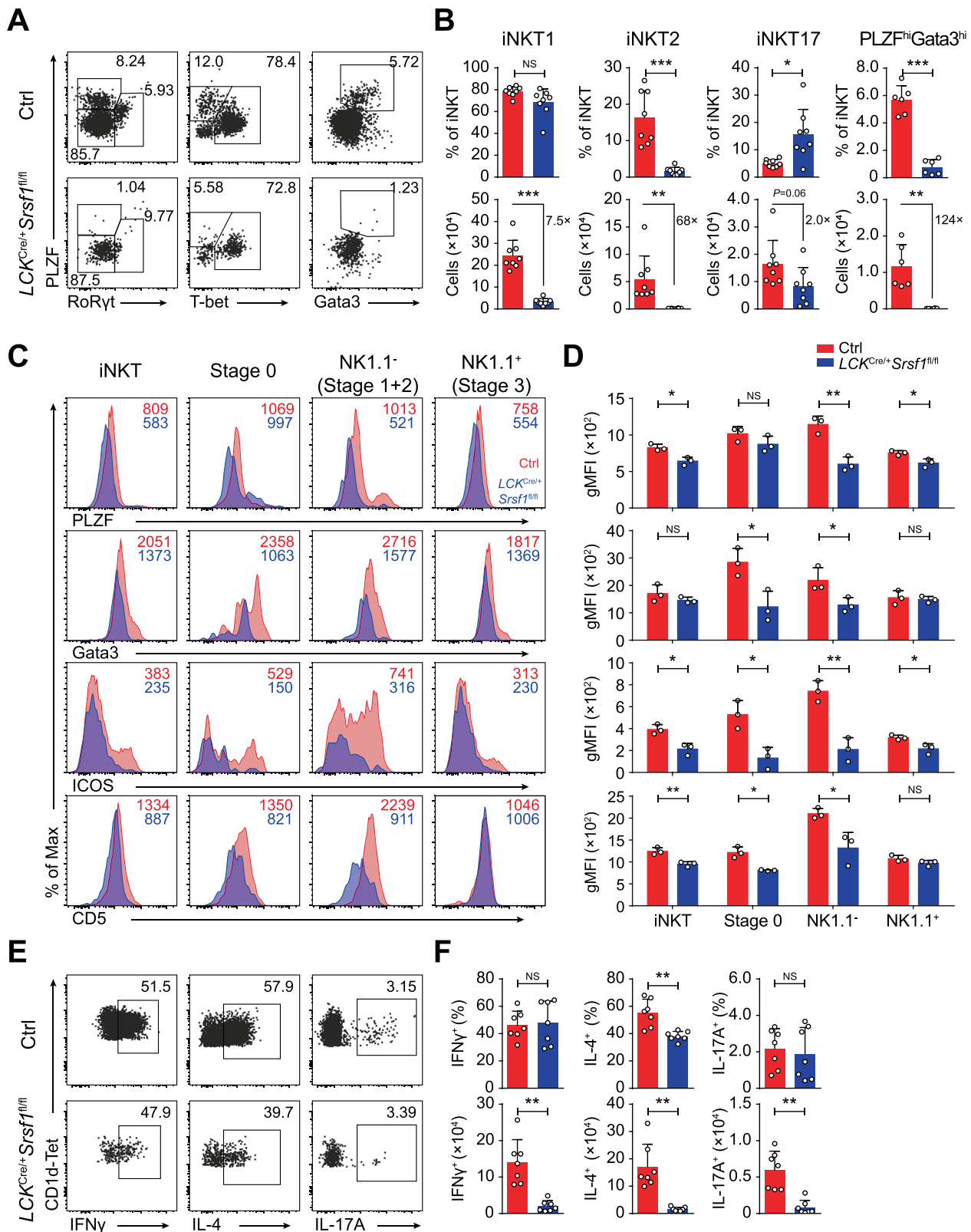


Fig. 3 SRSF1 is indispensable for iNKT cell functional differentiation. **A, B** Analysis of functional subsets in thymic iNKT cells. Representative dot plots (**A**) show iNKT1, iNKT2, iNKT17, and PLZF^{hi}Gata3^{hi} cells. The frequency and numbers of the indicated subsets are shown in (**B**) ($n \geq 6$). **C, D** Representative histograms (**C**) show the expression of PLZF, Gata3, ICOS, and CD5 in iNKT cells at distinct developmental stages by flow cytometry. The geometric mean fluorescence intensity (gMFI) of PLZF, Gata3, ICOS, and CD5 is shown in (**D**) ($n = 3$). **E, F** Representative dot plots (**E**) showing IFN γ ⁺, IL-4⁺, and IL-17A⁺ populations in thymic iNKT cells stimulated in vitro with PMA and ionomycin for 4 h. Frequency and numbers are shown in (**F**) ($n = 7$). Data were pooled from at least two independent experiments. Statistical significance was determined by unpaired two-sided Student's *t* test for normally distributed data, or an unpaired two-sided Welch's *t* test was used when variance between the groups was unequal. * $P < 0.05$; ** $P < 0.01$; *** $P < 0.001$; NS denotes not significant. Data are the mean \pm SD

SRSF1 is required for iNKT cell proliferation and survival

Given that blunted proliferation or increased apoptosis may account for rare iNKT cells, we then performed proliferation and apoptosis analyses on both DP and iNKT cells. BrdU incorporation in DP thymocytes and total iNKT cells exhibited no obvious differences between the genotypes of mice (Fig. 4A, B). However, when assessing the proportion of BrdU⁺ cells in distinct iNKT subsets, we found defective proliferation in thymic iNKT cells from stages 1 and 2 to stage 3 (CD24⁻ iNKT cells) but not in stage 0 (CD24⁺ iNKT cells), suggesting that SRSF1 affected iNKT cell proliferation in stages 1, 2, and 3 (Fig. 4A, B). Based on the Annexin V staining results, the SRSF1-deficient mice not only showed increased apoptosis of DP cells and total iNKT cells but also exhibited elevated apoptosis after stage 0 during iNKT cell differentiation (Fig. 4C, D). Accordingly, the expression of the antiapoptotic genes *Bcl2l1*, *Bcl2*, and *Mcl1* was lower, whereas the proapoptotic gene *Bid* was expressed at an aberrantly higher level in the SRSF1-deficient DP cells than in the control cells (Fig. 4E). In addition, we examined the expression of TCR signal response genes, which are also related to iNKT cell survival. The mRNA expression of *Zap70*, *Cd5*, and *Cd40lg* was dramatically decreased in the SRSF1-deficient iNKT cells, but *Egr2* and *Nr4a1* levels were not altered (Fig. 4F). Thus, our results indicated that SRSF1 maintains the survival of DP thymocytes and iNKT cells from stage 1 to stage 3.

SRSF1 deficiency impairs TCR α rearrangement

As indicated by the schematic map of TCR Va and Ja gene loci (Fig. 4G), the canonical iNKT TCR rearrangement joins Va14 to the distal Ja18 region and requires secondary rearrangements [43]. Increased apoptosis of DP thymocytes may account for impaired distal TCR α rearrangements due to the limited time for the generation of multiple DNA excision circles [44], which would in turn lead to fewer iNKT cells and skewing of the TCR repertoire. We then examined whether TCR α rearrangements were affected in the absence of SRSF1. The results demonstrated that both proximal and distal TCR α rearrangements were impaired in the SRSF1-deficient DP cells (Fig. 4H). Correspondingly, the TCR rearrangement-related gene *Dclre1c* showed downregulated expression and *Dntt* showed upregulated expression in the SRSF1-deficient DP thymocytes, but other key regulators, *Rag1*, *Rag2*, and *Lig4*, were not significantly changed (Fig. 4I).

SRSF1 globally alters the transcription of genes in DP cells

We next explored the underlying mechanism of SRSF1 regulation on iNKT cell development. DP thymocytes sorted from the *LCK^{Cre/+}Srsf1^{fl/fl}* and ctrl mice were used for RNA-seq. A total of 330 genes with upregulated and 579 genes with downregulated expression were identified in the SRSF1-deficient DP thymocytes (Fig. 5A). Gene Ontology (GO) enrichment analysis revealed that these differentially expressed genes (DEGs) were significantly enriched in the regulation of T cell differentiation, apoptosis, T-helper 2 cell differentiation, and RNA splicing (Fig. 5B). Among these DEGs, the expression of *Myb*, *Dclre1c*, *Itk*, and *Icos* was downregulated in the SRSF1-deficient DP thymocytes (Fig. 5C). We further validated these DEGs by qPCR and observed a significant reduction in *Myb* expression, which is involved in promoting early stages of iNKT cell development [23], in the SRSF1-deficient DP cells (Fig. 5D). The expression of iNKT-related genes, including the Tec kinases *Itk* and *Txk* and the costimulator *Icos*, was remarkably decreased in the SRSF1-deficient DP cells (Fig. 5D). These data revealed that loss of SRSF1 leads to aberrant expression of a set of gene transcription programs for iNKT cells.

To elucidate the underlying molecular mechanisms, we then screened SRSF1-controlled alternative splicing (AS) events. A total of 3,231 events, which could be classified into five

categories, were identified, and the majority of these AS events were skipped more in the DP thymocytes than the control thymocytes (Fig. 5E). To further strengthen the connection between SRSF1 and activation of the iNKT cell program, we analyzed DEGs from RNA-seq, AS events, and CLIP-seq of SRSF1 and found 111 DEGs with AS that were directly bound and regulated by SRSF1 (Fig. 5F). These findings thus suggested that SRSF1 controls the iNKT cell regulatory gene expression program through both direct and indirect regulatory mechanisms. In particular, *Myb* mRNA was differently spliced in the absence of SRSF1, reflecting the increased inclusion of exon 9A (Fig. 5G). Given that *Myb* deficiency leads to a severe reduction in iNKT cells in the thymus [23], we analyzed the published ChIP-seq data of *Myb* (GSE66122) and observed that a series of DEGs fall into *Myb*-binding genes (Fig. 5H and Supplementary Fig. 4A–D), which are related to iNKT cell differentiation, function, and survival. Based on our findings above, we speculated that *Myb* may serve as an essential downstream target of SRSF1 linked to iNKT cell differentiation.

SRSF1 regulates AS of *Myb* during iNKT cell development

We next confirmed that SRSF1 deficiency led to increased inclusion of exon 9A in both DP and iNKT cells by semiquantitative PCR (Fig. 6A). Moreover, qPCR results showed that the expression of the *Myb* short isoform (–Ex9A; encodes the p75 isoform, which is dominantly expressed in hematopoietic cells) was significantly decreased in the SRSF1-deficient DP and iNKT cells, whereas the expression of the *Myb* long isoform (+Ex9A; encodes the p89 isoform, which is a less abundant transcript) was notably elevated in iNKT cells (Fig. 6B). As a result, the reduced protein level of the p75 isoform in the SRSF1-deficient DP thymocytes was further confirmed by western blots (Fig. 6C). To further examine whether SRSF1 directly regulates the splicing of *Myb*, we generated a splicing minigene reporter containing *Myb* pre-mRNA in intron 9 with a WT/mutated SRSF1-binding site (named WT or Mut) (Fig. 6D). Overexpression of SRSF1 led to more skipping of exon 9A of mini*Myb*-WT (PSI changed from 23.1 to 4.7%), while impaired skipping was detected in exon 9A of mini*Myb*-Mut (PSI changed from 4.7 to 17.9%) (Fig. 6E). These data strongly supported the notion that SRSF1 directly binds to the alternative region of *Myb* to control its splicing.

Given that loss of the less abundant p89 isoform does not have any deleterious effects on hematopoiesis and development [45] and our results also indicated that SRSF1 tends to promote p75 isoform expression via AS, we thus questioned whether forced expression of *Myb*^{p75} could rectify the defects in iNKT cells. To achieve this goal, we employed bone marrow chimeric mice overexpressing *Myb*^{p75}, *Myb*^{p89}, or empty vector (EV). After 9 weeks of reconstitution, the *LCK^{Cre/+}Srsf1^{fl/fl}* DP cells with forced expression of *Myb*^{p75} exhibited less apoptosis than the cells transduced with EV retrovirus but not *Myb*^{p89} (Fig. 6F). Moreover, ectopic expression of the p75 isoform in the *LCK^{Cre/+}Srsf1^{fl/fl}* mice notably restored the proportion of iNKT cells (Fig. 6G). The expression of genes impaired by deactivated SRSF1, including *Myb*, *Bcl2l1*, *Gata3*, and *Itk*, was significantly rectified (Fig. 6H). Moreover, defective TCR α rearrangements were substantially rectified in the DP thymocytes transduced with the p75 retrovirus (Fig. 6I). However, overexpression of the p89 isoform did not result in phenotypic rescue in the SRSF1-deficient iNKT and DP cells (Fig. 6F–I). These findings strongly support that SRSF1-mediated splicing of *Myb* mRNA is a crucial regulatory event during iNKT cell development.

LCK^{Cre/+}Srsf1^{fl/fl} mice were highly tolerant of acute hepatic injury

As a key immune regulator, iNKT cells in the liver are tightly associated with multiple liver dysfunctions [46–49]. To test the role

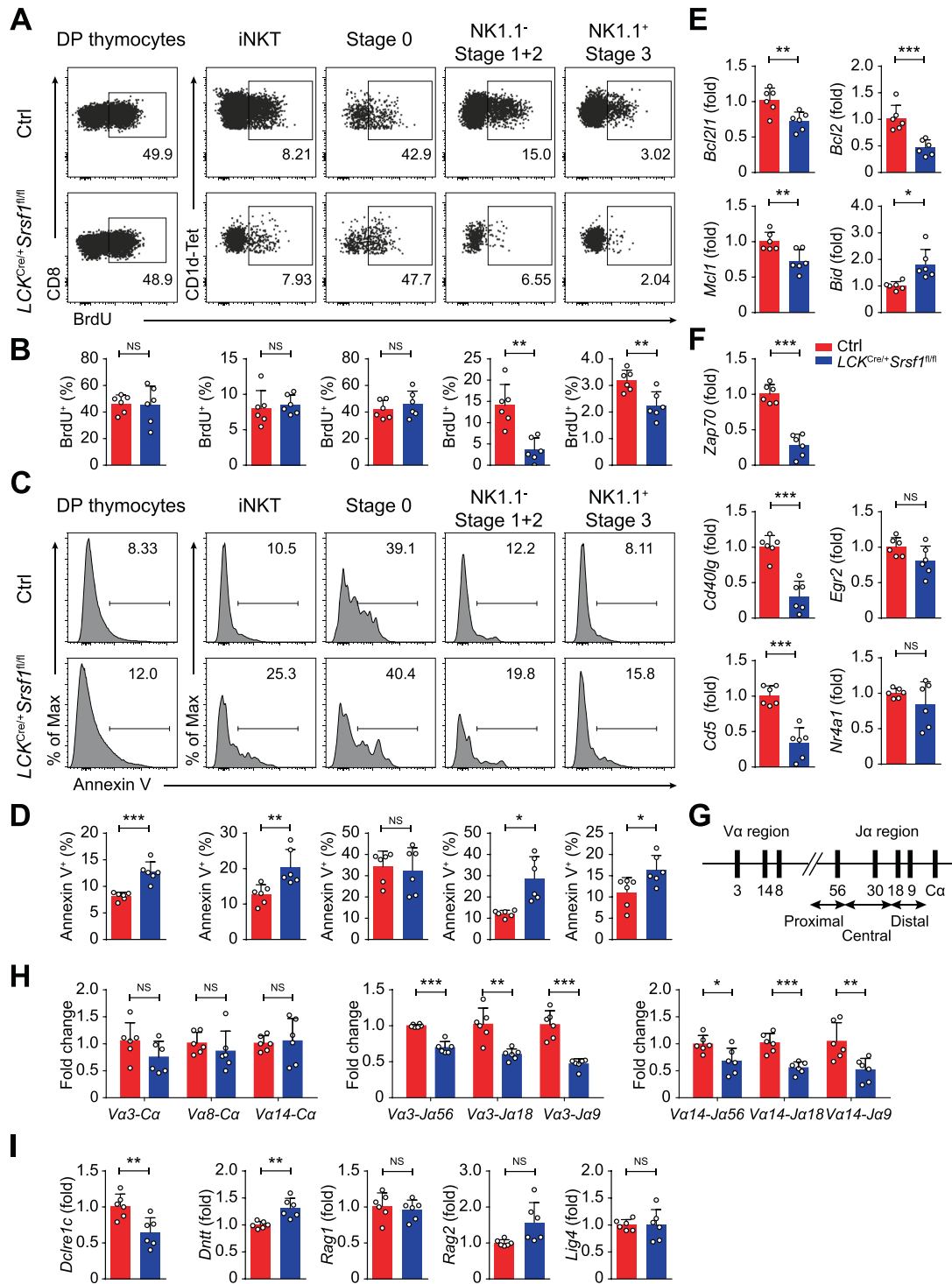


Fig. 4 SRSF1 deficiency impairs proliferation, survival, and TCR α rearrangement in iNKT and DP cells. **A, B** Proliferation assay. Representative dot plot (**A**) and frequency (**B**) of BrdU⁺ cells are shown in DP thymocytes and total; stage 0, NK1.1⁻ (stage 1 and 2), and NK1.1⁺ (stage 3) thymic iNKT cells, respectively ($n = 6$). **C, D** Apoptosis assay. Representative histogram (**C**) and frequency (**D**) of Annexin V⁺ cells are shown in DP thymocytes and total; stage 0, NK1.1⁻ (stage 1 and 2), and NK1.1⁺ (stage 3) thymic iNKT cells, respectively ($n = 6$). **E** Apoptosis-related gene expression in DP thymocytes. The relative expression of each transcript was normalized as described in Fig. 2A ($n = 6$). **F** Analysis of the expression of genes related to the TCR signaling response in thymic iNKT cells. The relative expression of each transcript was normalized accordingly as described in Fig. 2A ($n = 6$). **G** Schematic graph showing selected proximal, central, and distal V α and J α segments. **H** Analysis of transcripts of V α to J α rearrangements (constant α -region) segments and V α 14 and V α 3 rearrangements to J α 56, J α 18, or J α 9 by sorted DP thymocytes, presented relative to the expression of *Hprt1* transcript ($n = 6$). **I** qPCR analysis of rearrangement-related gene expression in DP thymocytes. The relative expression of each transcript was normalized accordingly as described above ($n = 6$). Data were pooled from at least three independent experiments. Statistical significance was determined by unpaired Student's *t* test for normally distributed data, or an unpaired two-sided Welch's *t* test when variance between the groups was unequal. * $P < 0.05$; ** $P < 0.01$; *** $P < 0.001$; NS denotes not significant. Data are the mean \pm SD

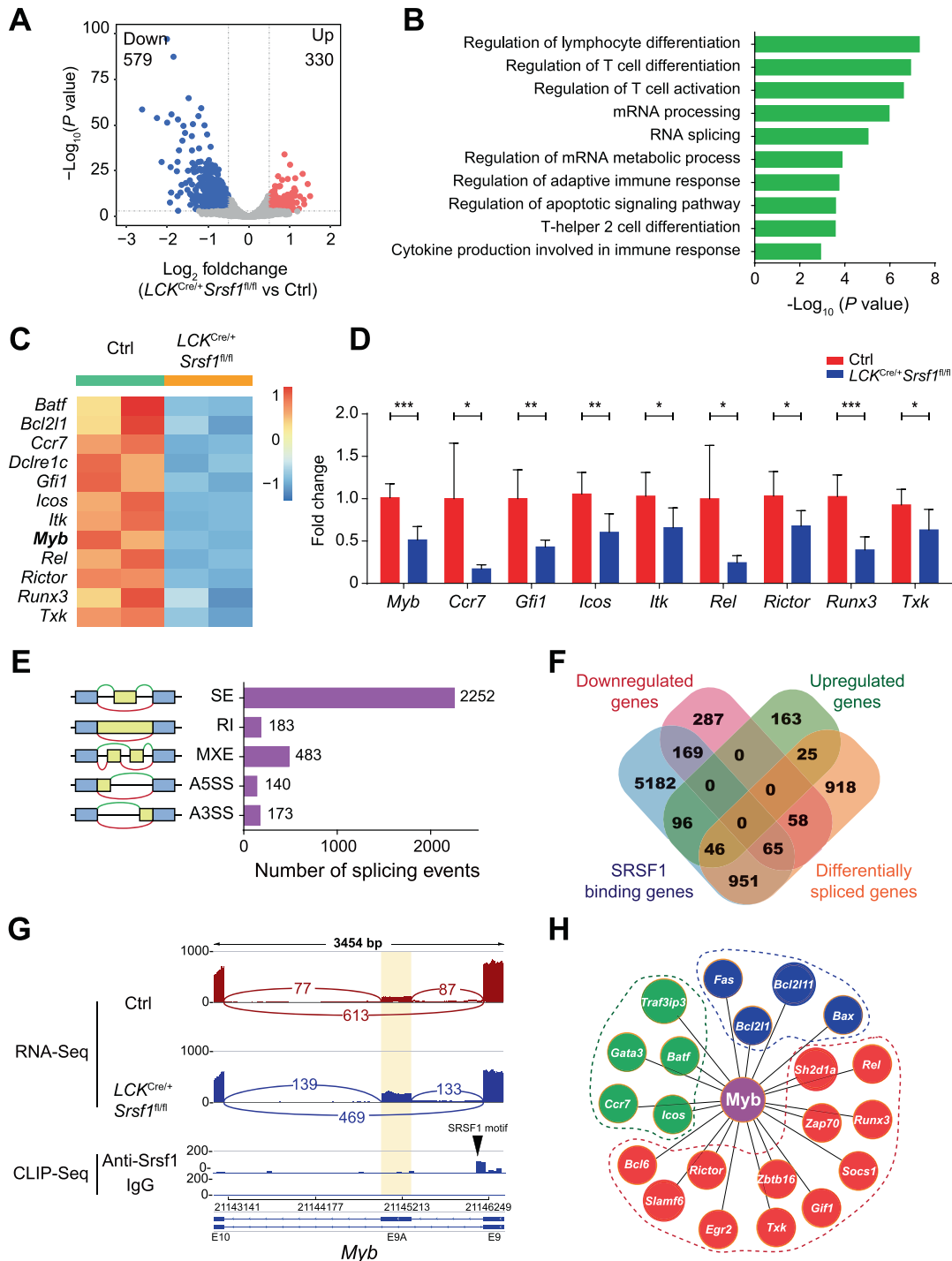


Fig. 5 SRSF1 modulates the expression of a series of iNKT cell-related genes. **A** Volcano plot depicting SRSF1-regulated genes in DP thymocytes. Differentially expressed genes (DEGs) were identified from *LCK*^{Cre/+} *Srsf1*^{fl/fl} versus ctrl samples (blue: downregulated; red: upregulated; gray: unchanged). **B** Representative Gene Ontology (GO) terms of the biological process categories enriched in DEGs. **C** Heatmap showing representative DEGs. **D** Quantification of selected DEGs in DP thymocytes. The relative expression of each transcript was normalized accordingly as described in Fig. 2A ($n = 6$). Data were pooled from three independent experiments. Statistical significance was determined by unpaired two-sided Student's t test for normally distributed data, or an unpaired two-sided Welch's t test was used when variance between the groups was unequal. * $P < 0.05$; ** $P < 0.01$; *** $P < 0.001$; NS denotes not significant. Data are the mean \pm SD. **E** Bar chart showing SRSF1-regulated alternative splicing (AS) events in DP thymocytes, classified into five categories: skipped exon (SE), retained intron (RI), mutually exclusive exon (MXE), alternative 5' splice site (A5SS), and alternative 3' splice site (A3SS). **F** Venn diagram showing the overlapping genes of DEGs in (A) and AS genes in (E) and SRSF1-binding genes in Fig. 1C. **G** Analysis of *Myb* expression and exon-exon junctions. "Sashimi plots" show read coverage and exon-exon junctions (numbers on arches indicate junction reads), and the alternative exons are shaded with yellow columns. The lower panel indicates SRSF1-binding sites identified by CLIP-seq. The black inverted triangle denotes the SRSF1-binding site in introns 9–10 of *Myb* pre-mRNA. **H** Analysis of *Myb*-binding genes (ChIP-seq, GSE66122) correlated with iNKT cells. Red dots represent iNKT cell development-related genes, green dots represent iNKT cell function- and effector differentiation-related genes, and blue dots denote apoptosis-related genes

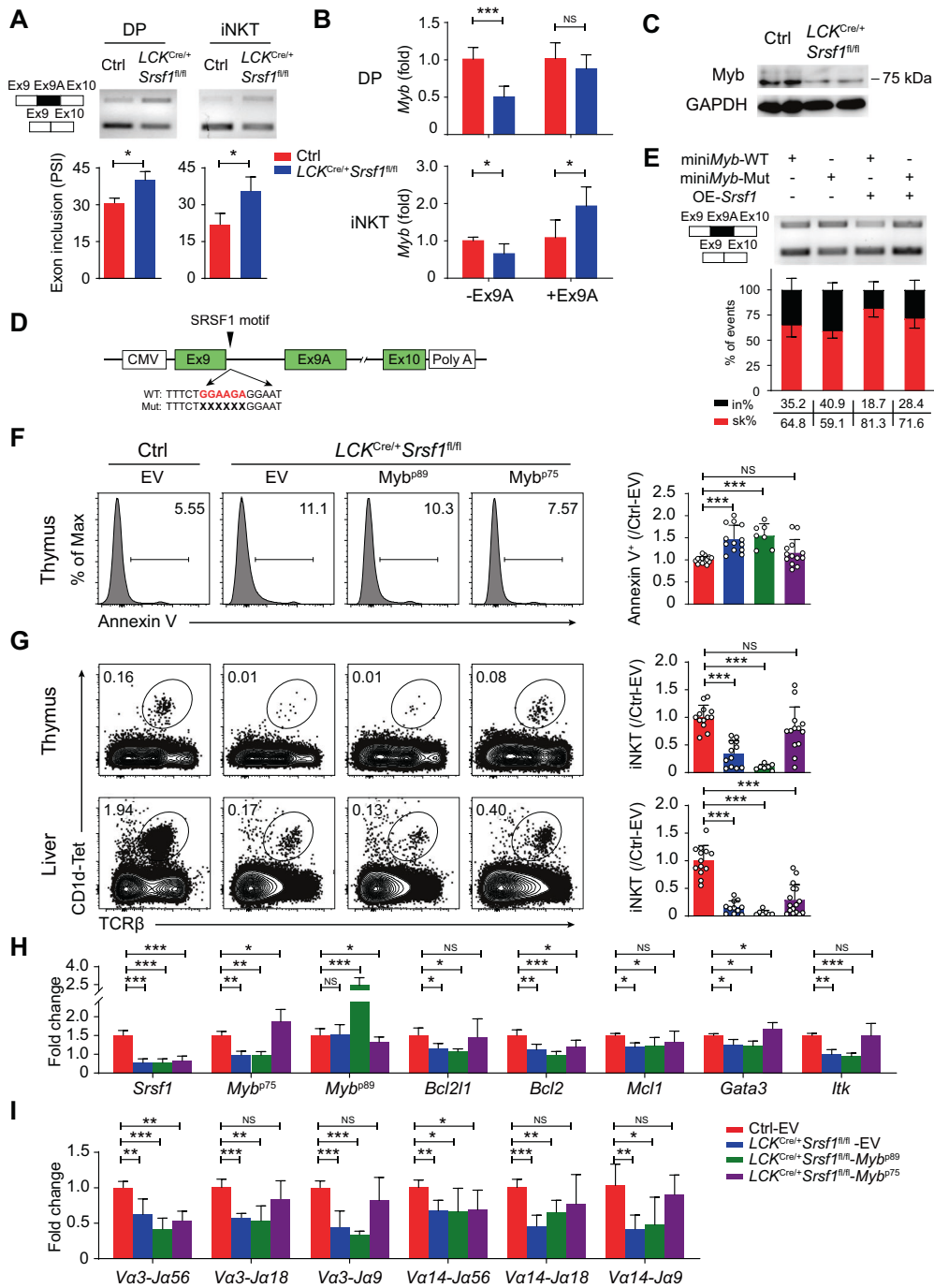
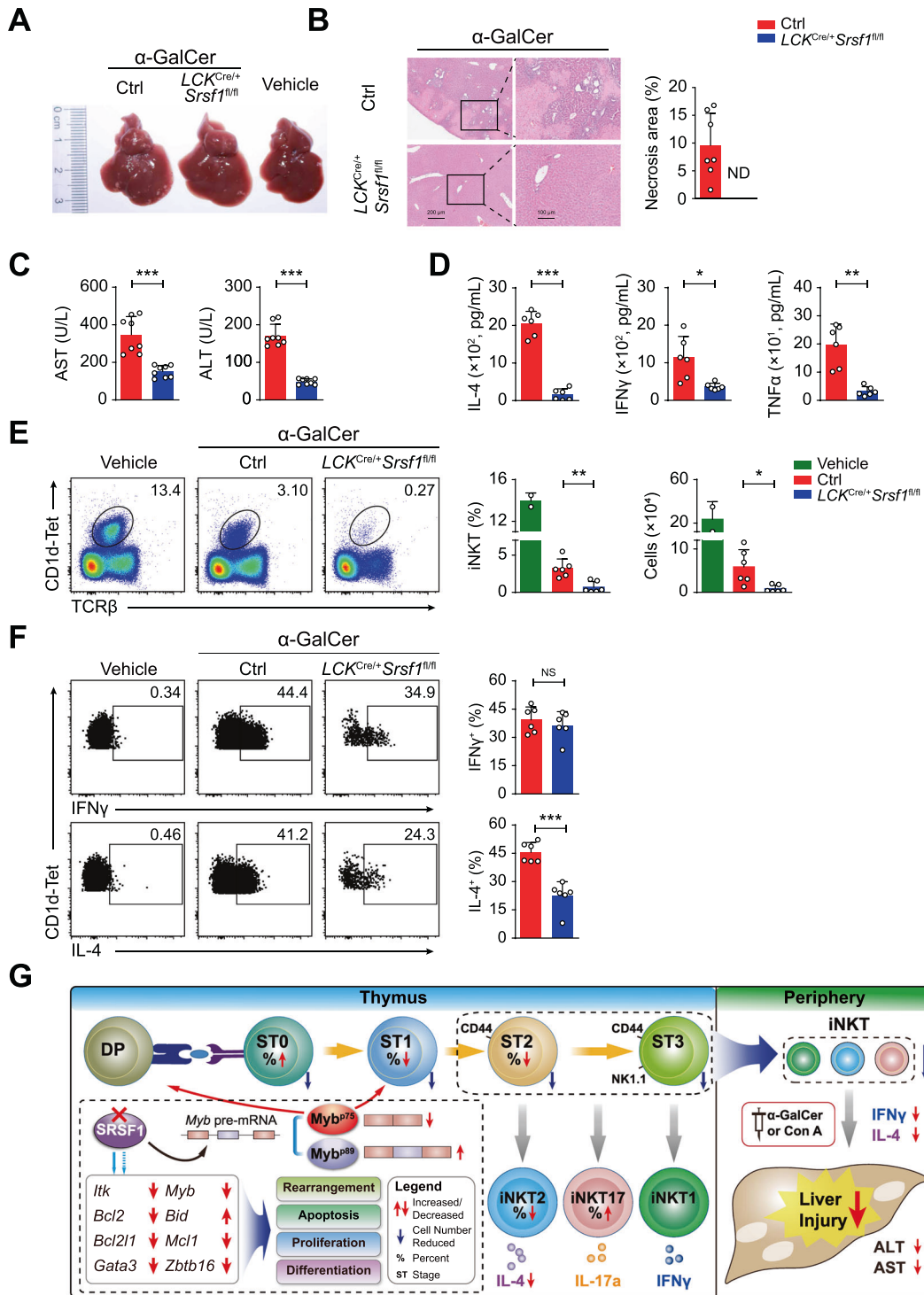


Fig. 6 SRSF1-mediated alternative splicing of *Myb* mRNA controls iNKT cell formation. **A** Semi-quantitative PCR validation of AS of *Myb* in DP and iNKT cells. The structure of PCR products is indicated schematically on the left. Alternative exon 9A is marked with black. Cumulative data are shown in the lower panel ($n = 3$). **B** qPCR analysis of the ratio of *Myb* transcripts with exon 9A (+Ex9A) and without exon 9A (-Ex9A) in DP and iNKT cells. The relative expression of each transcript was normalized accordingly as described in Fig. 2A ($n \geq 5$). **C** Western blot analysis of the protein level of Myb in DP thymocytes. **D** Graphical representation of *Myb* minigenes. The black arrow denotes the SRSF1-binding site in intron 9 of *Myb*. The potential SRSF1-binding motif is marked in red characters, and the specific deletion mutations are indicated with multiple "X". **E** Constructs with (WT) or without (Mut) SRSF1-binding site were applied for splicing assays with/without SRSF1 overexpression (OE) in HEK293T cells. The percentages of inclusion (in%, black) and skipping (sk%, red) within exon 9A of *Myb* transcripts are presented ($n = 5$). **F** Apoptosis of DP thymocytes in chimeras with forced expression of Myb^{p75} or Myb^{p89}. Annexin V⁺ donor-derived DP cells in thymi from recipients were detected. Representative dot plot and the ratio (the frequency of ctrl-EV was set to one) of Annexin V⁺ cells in DP thymocytes are shown ($n \geq 7$). **G** Analysis of iNKT cells in chimeras with forced expression of Myb^{p75} or Myb^{p89}. Donor-derived iNKT cells in thymi and livers from recipients were detected. Representative dot plot and the ratio (the frequency of ctrl-EV was set to one) of iNKT cells are shown ($n \geq 7$). **H, I** Analysis of the expression of genes impaired by ablation of SRSF1 (**H**) and TCR α rearrangement (**I**) in chimeric DP thymocytes. The relative expression of each transcript was normalized accordingly as described in Fig. 2A ($n = 5$). Data are pooled from at least three independent experiments. Statistical significance was determined by unpaired two-sided Student's *t* test for normally distributed data, or an unpaired two-sided Welch's *t* test was used when variance between the groups was unequal. For multiple comparisons, data were analyzed by one-way ANOVA. * $P < 0.05$; ** $P < 0.01$; *** $P < 0.001$; NS denotes not significant. Data are the mean \pm SD



of SRSF1 in the regulation of iNKT cell functions, we adopted α -GalCer-induced and Con A-induced hepatic injury models, which are well documented to experimentally resemble human autoimmune acute hepatitis [16, 49]. In the α -GalCer-induced groups, the ctrl mice exhibited aggravated liver injury compared with the $LCK^{Cre/+}Srsf1^{fl/fl}$ mice by liver morphology assays (Fig. 7A) and H&E staining (Fig. 7B). Two indices for liver damage, AST and ALT levels, were remarkably decreased in the serum of the $LCK^{Cre/+}Srsf1^{fl/fl}$ mice than the ctrl mice (Fig. 7C). The levels of IL-4, IFN γ , and TNF α in serum were higher in the ctrl mice than in the $LCK^{Cre/+}Srsf1^{fl/fl}$ mice (Fig. 7D). Correspondingly, a notable reduction in iNKT cells in the livers of the $LCK^{Cre/+}Srsf1^{fl/fl}$ mice was detected (Fig. 7E). Given that α -GalCer presented by CD1d provides specific iNKT-dependent activation, we further confirmed cytokine production at 2 h after α -GalCer stimulation in vivo. In accordance with the results in Fig. 3E, IL-4 expression was significantly decreased, but IFN γ was not, in iNKT cells from the SRSF1-deficient mice (Fig. 7F). Thus, we believe that both diminished iNKT numbers and defective IL-4 production in the SRSF1-deficient mice contributed to resistance to acute liver injury.

Similarly, after challenge with a low dose of Con A (15 mg/kg), the results were consistent with those in the α -GalCer-induced models (Supplementary Fig. 5A–E). Furthermore, when challenged with a lethal dose of Con A (30 mg/kg), all the ctrl mice died within 20 h, while approximately 40% of the $LCK^{Cre/+}Srsf1^{fl/fl}$ mice survived (Supplementary Fig. 5F). These results collectively demonstrated that conditional ablation of SRSF1 weakened pathologic symptoms in iNKT-related acute hepatic injury.

DISCUSSION

The regulation of iNKT cell development is a complicated process involved in a well-established transcription factor program [20], whereas the molecular mechanism by which iNKT cell differentiation is regulated post-transcriptionally is still unclear. In this study, we validated that RBP SRSF1 is crucial for iNKT cell development and cytokine production and affects multifunctional factors to form competent iNKT cells.

Previous studies have indicated that SRSF1 is essential for controlling proliferation- and survival-related events [50–53]. In terms of lymphocytes, conditional deletion of SRSF1 in T cells resulted in increased apoptosis due to decreased expression of the antiapoptotic gene *Bcl2l1* [52]. Similarly, SRSF1 deficiency accelerated apoptosis of both DP thymocytes and iNKT cells. Furthermore, SRSF1-deficient cells exhibited aberrantly increased expression of the proapoptotic gene *Bid* and decreased expression of the antiapoptotic genes *Bcl2l1*, *Bcl2*, and *Mcl1*, reflecting a shortened lifespan of these DP cells, which has effects on TCR α rearrangements of progenitors, ultimately resulting in a reduction in iNKT cell numbers [44]. Thus, the universal role of SRSF1 in cell survival is also essential for iNKT cell commitment.

Myb is essential for iNKT cell development and secretion of IL-4, a Th2-type cytokine [23, 54]. Similarly, we found that the SRSF1-deficient mice showed compromised iNKT cell generation and IL-4 production. By bioinformatics analysis, we found that 111 AS targets of SRSF1 were differentially expressed in DP thymocytes. Among them, we focused on the *Myb* gene, as its dominant mRNA product (short isoform Myb^{P75}) was remarkably switched to the exon-inclusion isoform (long isoform Myb^{P89}) in the absence of SRSF1, which was further validated by in vitro assays. Next, we selected the SRSF1-binding site (GA-enriched region) with the highest enrichment peak in introns 9–9A, which has been applied for mutagenesis in minigene analysis. Our results showed that fewer exon 9A skips were exhibited after this motif was mutated, indicating that this site located in intron 9–9A functions as an essential element to recruit SRSF1 for repression of exon 9 splicing with downstream exons. Given that specific effects on regulated splicing by one SR protein depend

on a complex set of relationships with multiple other SR proteins or RBPs, the precise mechanism of *Myb* splicing still needs to be further elucidated. We also found that ectopic expression of the short isoform of Myb^{P75} could partially rectify the defects of iNKT cells due to SRSF1 deficiency but not Myb^{P89}. These observations demonstrated that SRSF1-dependent AS of *Myb* is crucial for iNKT cell differentiation. We also observed that SRSF1 modulates the expression of *Dclre1c*, a key regulator involved in remodeling and repair of break ends during V(D)J recombination [55]. Accordingly, the SRSF1-deficient DP cells exhibited defective TCR α rearrangements, which have also been observed in *Myb*-deficient DP cells [23]. In addition, we observed that SRSF1 deficiency impaired the expression of a series of iNKT transcription factors (TFs). For instance, SRSF1 indirectly controls the expression of PLZF, a master regulator of iNKT cell development [21, 22]. SRSF1 also maintains *Gata3* expression, and the SRSF1-deficient mice phenocopied *Gata3* deficiency, with a reduction in CD4⁺ iNKT cells and iNKT2 cell differentiation [8, 26]. Thus, SRSF1 directly or indirectly modulates the gene network involved in sustaining iNKT cell development. Furthermore, our recent study revealed that SRSF1 safeguards the late-stage development of conventional T cells by directly binding and regulating *Irf7* and *Ii27ra* expression, which is critical in the response to type I interferon signaling during T cell terminal maturation [56]. These findings collectively suggested that SRSF1 serves as a critical post-transcriptional regulator in both conventional T and iNKT cell intrathymic development by modulating distinct targets in a stage-specific manner.

SRSF1 exerted oncogenic roles via the control of AS of cancer-related genes overexpressed in human tumors. The liver harbors many iNKT cells, which are closely related to liver dysfunction [46]. Con A-induced liver injury in mice is regarded as a classic model to mimic pathogenic mechanisms and pathological changes in patients with liver inflammatory diseases [14, 16]. The α -GalCer-induced hepatitis mouse model with CD1d shows specific iNKT-dependent activation that resembles human autoimmune acute hepatitis [49]. When challenged with Con A or α -GalCer, the SRSF1-deficient mice showed more resistance than the ctrl mice. In addition, the SRSF1-deficient mice exhibited attenuated cytokine production, including that of IL-4, IFN γ , and TNF α , due to fewer iNKT cells and defects in IL-4 production by iNKT cells. Based on these findings, our study sheds light on SRSF1 as a potential clinical therapeutic target for diagnosis and therapy.

In summary, SRSF1 acts as a key post-transcriptional regulator to maintain TCR α arrangement, proliferation, survival, and functional differentiation of iNKT cells. By utilizing multipronged mechanisms, SRSF1 controls the expression of genes involved in iNKT differentiation and survival, including *Myb*, *Itk*, *Gata3*, *Zbtb16*, *Bcl2*, *Bcl2l1*, *Mcl1*, *Bid*, and TCR signaling. Furthermore, SRSF1-deficient mice were highly tolerant of induced liver injury, which is tightly associated with impaired iNKT cell numbers and function (Fig. 7G). The induced animal models verified the relevance between SRSF1 expression level and liver injury. Thus, our study not only provides new insight into SRSF1-dependent post-transcriptional regulation in iNKT cells but also sheds light on the clinical diagnosis and therapy of iNKT-related liver diseases.

REFERENCES

- Pellicci DG, Koay HF, Berzins SP. Thymic development of unconventional T cells: how NKT cells, MAIT cells and gammadelta T cells emerge. *Nat Rev Immunol*. 2020;12:756–70.
- Lantz O, Bendelac A. An invariant T cell receptor alpha chain is used by a unique subset of major histocompatibility complex class I-specific CD4⁺ and CD4-8- T cells in mice and humans. *J Exp Med*. 1994;180:1097–106.
- Adachi Y, Koseki H, Zijlstra M, Taniguchi M. Positive selection of invariant V alpha 14+ T cells by non-major histocompatibility complex-encoded class I-like

- molecules expressed on bone marrow-derived cells. *Proc Natl Acad Sci USA*. 1995;92:1200–4.
4. Kawano T, Cui J, Koezuka Y, Toura I, Kaneko Y, Motoki K, et al. CD1d-restricted and TCR-mediated activation of α 14 NKT cells by glycosylceramides. *Science*. 1997;278:1626–9.
 5. Beckman EM, Porcelli SA, Morita CT, Behar SM, Furlong ST, Brenner MB. Recognition of a lipid antigen by CD1-restricted α 14 NKT cells. *Nature*. 1994;372:691–4.
 6. Bendelac A, Savage PB, Teyton L. The biology of NKT cells. *Annu Rev Immunol*. 2007;25:297–336.
 7. Godfrey DI, Berzins SP. Control points in NKT-cell development. *Nat Rev Immunol*. 2007;7:505–18.
 8. Lee YJ, Holzapfel KL, Zhu J, Jameson SC, Hogquist KA. Steady-state production of IL-4 modulates immunity in mouse strains and is determined by lineage diversity of iNKT cells. *Nat Immunol*. 2013;14:1146–54.
 9. Harsha Krovi S, Zhang J, Michaels-Foster MJ, Brunetti T, Loh L, Scott-Browne J, et al. Thymic iNKT single cell analyses unmask the common developmental program of mouse innate T cells. *Nat Commun*. 2020;11:6238.
 10. Baranek T, Lebrigand K, de Amat Herbozo C, Gonzalez L, Bogard G, Dietrich C, et al. High dimensional single-cell analysis reveals iNKT cell developmental trajectories and effector fate decision. *Cell Rep*. 2020;32:108116.
 11. Coquet JM, Chakravarti S, Kyparissoudis K, McNab FW, Pitt LA, McKenzie BS, et al. Diverse cytokine production by NKT cell subsets and identification of an IL-17-producing CD4-NK1.1- NKT cell population. *Proc Natl Acad Sci USA*. 2008;105:11287–92.
 12. Brennan PJ, Brigl M, Brenner MB. Invariant natural killer T cells: an innate activation scheme linked to diverse effector functions. *Nat Rev Immunol*. 2013;13:101–17.
 13. Crosby CM, Kronenberg M. Tissue-specific functions of invariant natural killer T cells. *Nat Rev Immunol*. 2018;18:559–74.
 14. Dong Z, Wei H, Sun R, Tian Z. The roles of innate immune cells in liver injury and regeneration. *Cell Mol Immunol*. 2007;4:241–52.
 15. Wang H, Feng D, Park O, Yin S, Gao B. Invariant NKT cell activation induces neutrophil accumulation and hepatitis: opposite regulation by IL-4 and IFN- γ . *Hepatology*. 2013;58:1474–85.
 16. Heymann F, Hamesch K, Weiskirchen R, Tacke F. The concanavalin A model of acute hepatitis in mice. *Lab Anim*. 2015;49(1 Suppl):12–20.
 17. Liew PX, Lee WY, Kubes P. iNKT cells orchestrate a switch from inflammation to resolution of sterile liver injury. *Immunity*. 2017;47:752–65 e5.
 18. Shissler SC, Webb TJ. The ins and outs of type I iNKT cell development. *Mol Immunol*. 2019;105:116–30.
 19. Godfrey DI, Stankovic S, Baxter AG. Raising the NKT cell family. *Nat Immunol*. 2010;11:197–206.
 20. Gapin L. Development of invariant natural killer T cells. *Curr Opin Immunol*. 2016;39:68–74.
 21. Kovalovsky D, Uche OU, Eladad S, Hobbs RM, Yi W, Alonzo E, et al. The BTB-zinc finger transcriptional regulator PLZF controls the development of invariant natural killer T cell effector functions. *Nat Immunol*. 2008;9:1055–64.
 22. Savage AK, Constantinides MG, Han J, Picard D, Martin E, Li B, et al. The transcription factor PLZF directs the effector program of the NKT cell lineage. *Immunity*. 2008;29:391–403.
 23. Hu T, Simmons A, Yuan J, Bender TP, Alberola-Ila J. The transcription factor c-Myb primes CD4⁺CD8⁺ immature thymocytes for selection into the iNKT lineage. *Nat Immunol*. 2010;11:435–41.
 24. Wikenheiser DJ, Stumhofer JS. ICOS co-stimulation: friend or foe? *Front Immunol*. 2016;7:304.
 25. Akbari O, Stock P, Meyer EH, Freeman GJ, Sharpe AH, Umetsu DT, et al. ICOS/ICOSL interaction is required for CD4⁺ invariant NKT cell function and homeostatic survival. *J Immunol*. 2008;180:5448–56.
 26. Kim PJ, Pai SY, Brigl M, Besra GS, Gumperz J, Ho IC. GATA-3 regulates the development and function of invariant NKT cells. *J Immunol*. 2006;177:6650–9.
 27. Seiler MP, Mathew R, Liszewski MK, Spooner CJ, Barr K, Meng F, et al. Elevated and sustained expression of the transcription factors Egr1 and Egr2 controls NKT lineage differentiation in response to TCR signaling. *Nat Immunol*. 2012;13:264–71.
 28. Townsend MJ, Weinmann AS, Matsuda JL, Salomon R, Farnham PJ, Biron CA, et al. T-bet regulates the terminal maturation and homeostasis of NK and α 14 NKT cells. *Immunity*. 2004;20:477–94.
 29. Weinreich MA, Odumade OA, Jameson SC, Hogquist KA. T cells expressing the transcription factor PLZF regulate the development of memory-like CD8⁺ T cells. *Nat Immunol*. 2010;11:709–16.
 30. Li J, Wu D, Jiang N, Zhuang Y. Combined deletion of Id2 and Id3 genes reveals multiple roles for E proteins in invariant NKT cell development and expansion. *J Immunol*. 2013;191:5052–64.
 31. Li J, Roy S, Kim YM, Li S, Zhang B, Love C, et al. Id2 collaborates with Id3 to suppress invariant NKT and innate-like tumors. *J Immunol*. 2017;198:3136–48.
 32. Dvinge H, Kim E, Abdel-Wahab O, Bradley RK. RNA splicing factors as oncoproteins and tumour suppressors. *Nat Rev Cancer*. 2016;16:413–30.
 33. Jeong SSR. Proteins: binders, regulators, and connectors of RNA. *Mol Cells*. 2017;40:1–9.
 34. Das S, Krainer AR. Emerging functions of SRSF1, splicing factor and oncoprotein, in RNA metabolism and cancer. *Mol Cancer Res*. 2014;12:1195–204.
 35. Xu X, Yang D, Ding JH, Wang W, Chu PH, Dalton ND, et al. ASF/SF2-regulated CaMKII δ alternative splicing temporally reprograms excitation-contraction coupling in cardiac muscle. *Cell*. 2005;120:59–72.
 36. Hennes T, Hagen FK, Tabak LA, Marth JD. T-cell-specific deletion of a polypeptide N-acetylgalactosaminyl-transferase gene by site-directed recombination. *Proc Natl Acad Sci USA*. 1995;92:12070–4.
 37. Liu J, Cui Z, Wang F, Yao Y, Yu G, Liu J, et al. Lrp5 and Lrp6 are required for maintaining self-renewal and differentiation of hematopoietic stem cells. *FASEB J*. 2019;33:5615–25.
 38. Kim TJ, Park G, Kim J, Lim SA, Kim J, Im K, et al. CD160 serves as a negative regulator of NKT cells in acute hepatic injury. *Nat Commun*. 2019;10:3258.
 39. Yao Y, Guo W, Chen J, Guo P, Yu G, Liu J, et al. Long noncoding RNA Malat1 is not essential for T cell development and response to LCMV infection. *RNA Biol*. 2018;15:1477–86.
 40. Bedel R, Berry R, Malleveay T, Matsuda JL, Zhang J, Godfrey DI, et al. Effective functional maturation of invariant natural killer T cells is constrained by negative selection and T-cell antigen receptor affinity. *Proc Natl Acad Sci USA*. 2014;111:E119–28.
 41. Yu S, Zhou X, Steinke FC, Liu C, Chen SC, Zagorodna O, et al. The TCF-1 and LEF-1 transcription factors have cooperative and opposing roles in T cell development and malignancy. *Immunity*. 2012;37:813–26.
 42. Godfrey DI, MacDonald HR, Kronenberg M, Smyth MJ, Van Kaer L. NKT cells: what's in a name? *Nat Rev Immunol*. 2004;4:231–7.
 43. Guo J, Hawwari A, Li H, Sun Z, Mahanta SK, Littman DR, et al. Regulation of the TCR α repertoire by the survival window of CD4⁺CD8⁺ thymocytes. *Nat Immunol*. 2002;3:469–76.
 44. Das R, Sant'Angelo DB, Nichols KE. Transcriptional control of invariant NKT cell development. *Immunol Rev*. 2010;238:195–215.
 45. Baker SJ, Kumar A, Reddy EP. p89c-Myb is not required for fetal or adult hematopoiesis. *Genesis*. 2010;48:309–16.
 46. Zhu S, Zhang H, Bai L. NKT cells in liver diseases. *Front Med*. 2018;12:249–61.
 47. Bandyopadhyay K, Marrero I, Kumar V. NKT cell subsets as key participants in liver physiology and pathology. *Cell Mol Immunol*. 2016;13:337–46.
 48. Huang W, He W, Shi X, He X, Dou L, Gao Y. The role of CD1d and MR1 restricted T cells in the liver. *Front Immunol*. 2018;9:2424.
 49. Dennert G, Aswad F. The role of NKT cells in animal models of autoimmune hepatitis. *Crit Rev Immunol*. 2006;26:453–73.
 50. Anczukow O, Rosenberg AZ, Akerman M, Das S, Zhan L, Karni R, et al. The splicing factor SRSF1 regulates apoptosis and proliferation to promote mammary epithelial cell transformation. *Nat Struct Mol Biol*. 2012;19:220–8.
 51. Zhou X, Wang R, Li X, Yu L, Hua D, Sun C, et al. Splicing factor SRSF1 promotes gliomagenesis via oncogenic splice-switching of MYO1B. *J Clin Invest*. 2019;129:676–93.
 52. Katsuyama T, Martin-Delgado IJ, Krishfield SM, Kyttaris VC, Moulton VR. Splicing factor SRSF1 controls T cell homeostasis and its decreased levels are linked to lymphopenia in systemic lupus erythematosus. *Rheumatology*. 2020;59:2146–55.
 53. Li X, Wang J, Manley JL. Loss of splicing factor ASF/SF2 induces G2 cell cycle arrest and apoptosis, but inhibits internucleosomal DNA fragmentation. *Genes Dev*. 2005;19:2705–14.
 54. Nakata Y, Brignier AC, Jin S, Shen Y, Rudnick SI, Sugita M, et al. c-Myb, Menin, GATA-3, and MLL form a dynamic transcription complex that plays a pivotal role in human T helper type 2 cell development. *Blood*. 2010;116:1280–90.
 55. Rooney S, Sekiguchi J, Zhu C, Cheng HL, Manis J, Whitlow S, et al. Leaky Scid phenotype associated with defective V(D)J coding end processing in Artemis-deficient mice. *Mol Cell*. 2002;10:1379–90.
 56. Qi Z, Wang F, Yu G, Wang D, Yao Y, You M, et al. SRSF1 serves as a critical posttranscriptional regulator at the late stage of thymocyte development. *Sci Adv*. 2021;16:eabf0753.

ACKNOWLEDGEMENTS

This work was supported in part by grants from the National Key Research and Development Program of China (2017YFA0104401), the National Natural Scientific Foundation of China (32130039, 31970831, and 31630038), and the Project for Extramural Scientists of State Key Laboratory of Agrobiotechnology from China Agricultural University (2021SKLAB6-3, 2021SKLAB6-4, 2019SKLAB6-6, and 2019SKLAB6-7).

AUTHOR CONTRIBUTIONS

Jingjing L., M.Y., and C.J. performed the major experiments and analyzed the data; M.Y., Z.W., and F.W. analyzed the high-throughput data; D.W., Z.Q., Y.Y., G.Y., Z.S., W.G., Juanjuan L., S.L., Y.J., and T.Z. assisted with the overall experiments; S.Y. designed and supervised the experiments with constructive suggestions from H.-H.X. and Y.X.; Y.Y., Jingjing L., and S.Y. wrote the manuscript with revisions from all authors.

COMPETING INTERESTS

The authors declare no competing interests.

ADDITIONAL INFORMATION

Supplementary information The online version contains supplementary material available at <https://doi.org/10.1038/s41423-021-00766-w>.

Correspondence and requests for materials should be addressed to Shuyang Yu.

Reprints and permission information is available at <http://www.nature.com/reprints>